

Weak Ferromagnetism and Spin Glass in κ -(BEDT-TTF)₂Hg(SCN)₂Br

M. Hemmida,¹ H.-A. Krug von Nidda,² B. Miksch,¹ L. L. Samoilenko,¹
A. Pustogow,¹ J. Schlueter,³ A. Loidl,² and M. Dressel¹

¹*Physikalisches Institut, Universität Stuttgart, Pfaffenwaldring 57, 70550 Stuttgart, Germany*

²*Experimental Physics V, Center for Electronic Correlations and Magnetism,
Universität Augsburg, 86135 Augsburg, Germany*

³*Division of Materials research, National Science Foundation, Arlington, VA 22230, and
Material Science Division, Argonne National Laboratory, Argonne, Illinois 60439-4831, U.S.A.*

(Dated: June 22, 2019)

Since the first observation of weak ferromagnetism in the charge-transfer salt κ -(BEDT-TTF)₂-Cu[N(CN)₂]Cl [U. Welp *et al.*, Phys. Rev. Lett. **69**, 840 (1992)], no further evidence of ferromagnetism in this class of organic materials has been reported. Here we present static and dynamic spin susceptibility measurements on κ -(BEDT-TTF)₂Hg(SCN)₂Br revealing weak ferromagnetism below $T_{WF} \approx 20$ K. We suggest that frustrated spins in the molecular dimers suppress long-range order, forming a spin-glass ground state in the insulating phase.

PACS numbers: 33.35.+r, 75.40.Gb, 76.30.-v, 75.50.Gg

In the last decades, the search for ferromagnetism in low-dimensional organic charge-transfer salts has continuously attracted attention in physics, chemistry, and materials sciences. However, pure ferromagnetic organic π -electron systems containing only s - and p -valence electrons are still rare and their synthesis is a challenging problem [1–6], while in inorganic magnetic materials ferromagnetism usually arises from transition metals or transition-metal ions ($3d$, $4f$), which in case of direct exchange may fulfill the Stoner criterion or in case of indirect exchange are subject to Goodenough-Kanamori-Anderson rules or Zener double exchange [7].

The organic radical salts κ -(BEDT-TTF)₂ X , where BEDT-TTF is the abbreviation of bis-(ethylenedithio)-tetrathiafulvalene, consist of alternating layers of the electron donor BEDT-TTF and electron acceptor X . In the κ -phase crystal structure the BEDT-TTF molecules stack in pairs as depicted in Fig. 1. Here the (BEDT-TTF)₂ dimers are arranged in a two-dimensional structure rather than in a chain type. Within the BEDT-TTF layers, the molecular dimers are close to each other, allowing substantial overlap of the molecular orbitals. Since one electron is transferred from each (BEDT-TTF)₂ dimer to the anion, the conduction band is half-filled. This implies that these organic compounds are metallic enabling nearly isotropic electron motion within the layer; perpendicularly to the plane the resistivity is larger by more than one order of magnitude [8–10].

The BEDT-TTF-based salts can be easily tuned by hydrostatic and uniaxial pressure, deuteration, or chemical substitution such that a wide range of electronic phases is obtained including paramagnetic, antiferromagnetic, spin-liquid, and superconducting ground states [11]. The best studied examples are the κ -(BEDT-TTF)₂ X compounds, where X denotes the anion such as Cu[N(CN)₂]Cl[−], Cu[N(CN)₂]Br[−] or Cu₂(CN)₃[−]. Since the inter-dimer transfer integral between the π orbitals

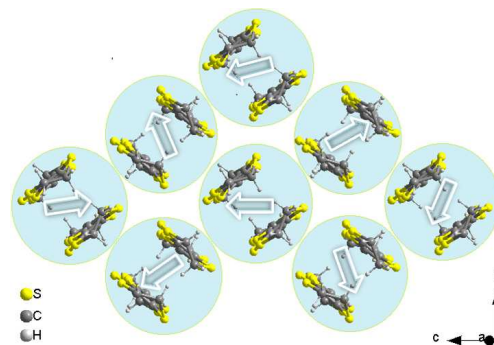


FIG. 1: Top view of the dimerized BEDT-TTF molecules of κ -(BEDT-TTF)₂Hg(SCN)₂Br; each dimer has one spin. The dimer pattern can be modeled by an almost isosceles triangular lattice that is characterized by frustration effects. An artistic view of the spin arrangement illustrates that below the metal-insulator transition at $T_{MI} = 80$ K, spin frustration becomes dominant and suppresses the magnetic order. Here all spins are localized and have an antiferromagnetic coupling.

(≈ 0.05 eV) is comparable to the on-site Coulomb repulsion (≈ 0.3 eV), electronic correlations cannot be neglected [12, 13]. In recent years substantial efforts were devoted to the study of the Mott metal-insulator transition in these compounds.

Here we want to draw the attention to the family of κ -BEDT-TTF salts with mercury-based anions [14] where the ratio of Coulomb interaction and transfer integrals is significantly smaller; correspondingly the inter-dimer coupling is more effective [15, 16]. Electrical resistivity measurements evidence that κ -(BEDT-TTF)₂Hg(SCN)₂Br undergoes a transition from a metallic to an insulating phase upon cooling below $T_{MI} = 80$ K [16, 17]; the origin of the transition, however, is still under debate. It was demonstrated [15] that the isostructural sister compound κ -(BEDT-TTF)₂Hg(SCN)₂Cl enters a charge-ordered state at $T_{CO} = 30$ K. Compre-

hensive transport, dielectric, and optical investigations of the present compound κ -(BEDT-TTF)₂Hg(SCN)₂Br, however, do not find any evidence of charge order or structural changes [16]. This might resemble the Mott insulators κ -(BEDT-TTF)₂Cu[N(CN)₂]Cl, κ -(BEDT-TTF)₂Cu₂(CN)₃ or κ -(BEDT-TTF)₂Ag₂(CN)₃, where also no indication of charge order is seen [18, 19], yet the resistivity jump in κ -(BEDT-TTF)₂Hg(SCN)₂Br is rather abrupt.

In an early electron spin resonance (ESR) characterization of hydrogenated and deuterated κ -(BEDT-TTF)₂-Hg(SCN)₂Br reported two decades ago [20], a first-order phase transition was supposed in the hydrogenated compound around 100 K and associated with localization of electrons on the (BEDT-TTF)₂ dimers; a transition of semiconductor-semiconductor type was suggested for the deuterated compound with possible magnetic ordering. However, low-temperature x-ray diffraction studies did not reveal any evidence of structural changes refuting a first-order transition [16]. Based on detailed magnetization and ESR investigations we could now unveil a weak ferromagnetic state at low temperatures. There is no long-range order, instead the frustrated spins form a spin glass state.

Single crystals of κ -(BEDT-TTF)₂Hg(SCN)₂Br were prepared following the synthesis method of Lyubovskaya and collaborators [21, 22]. It is important to note that the stable divalent state of the Hg²⁺ ions (5d¹⁰) is non-magnetic and, hence, magnetism will not be hampered by any kind of valence changes like in the case of the Cu-based BEDT-TTF salts; besides a majority of Cu⁺ ions (3d¹⁰) those crystals usually contain Cu²⁺ ions (3d⁹), which can strongly influence the magnetic properties [23].

Magnetization measurements were performed at temperatures $2 \leq T \leq 300$ K using a superconducting quantum interference device (SQUID) MPMS XL (Quantum Design). As the mass of the single crystals under investigation is only about 1 mg, the magnetization data had to be corrected by subtraction of the diamagnetic background of the sample holder, measured beforehand under the same conditions. The diamagnetic contribution of κ -(BEDT-TTF)₂Hg(SCN)₂Br is estimated as $\chi_{\text{dia}} \approx -5 \times 10^{-4}$ emu/mol.

The ESR measurements were performed in a Bruker ELEXSYS E500-CW X-band spectrometer at 9.36 GHz frequency equipped with a standard continuous He-gas flow cryostat working in the temperature range down to 4.2 K. The samples were fixed in a quartz tube by parafin.

In the whole temperature regime, the ESR spectra of κ -(BEDT-TTF)₂Hg(SCN)₂Br, displayed in Fig. 2, are well described by the field derivative of a single Lorentz line. The signal results from dipole transitions between the Zeeman levels between the conduction electron spins. Below $T \approx 20$ K comparison of zero-field cooled (ZFC) and field cooled (FC) measurements reveals a slight res-

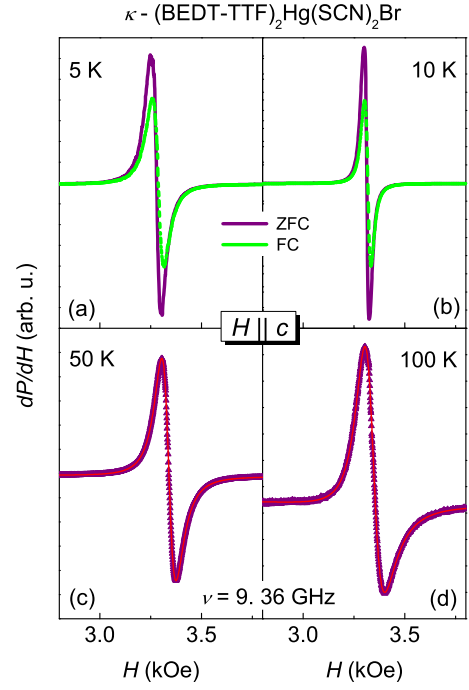


FIG. 2: ESR spectra, i.e. field derivative of absorbed power, of κ -(BEDT-TTF)₂Hg(SCN)₂Br taken at X-band frequency for selected temperatures and $H \parallel c$ as indicated. Zero-field cooled (ZFC) and field cooled (FC) measurements (green) are depicted in (a) and (b). The red solid lines, shown in (c) and (d) correspond to a fit by the field derivative of a Lorentz and Dyson line, respectively.

onance shift, line broadening and decrease of the amplitude for the FC case [Fig. 2(a,b)]. This is a well-known aspect of a spin-glass behavior (see e.g. Ref. 24). Above $T \approx 80$ K the system becomes metallic and especially for the case that the microwave field is applied perpendicular to the conductive planes, the Lorentz line transforms to an asymmetrical shape (Dysonian) (Fig. 2(d)). This is due to the skin effect, which appears in conductive compounds because of the interaction between the applied microwave field and mobile charge carriers. For the microwave field applied perpendicular to the conductive planes, shielding currents are induced in these conductive planes that drive electric and magnetic microwave components out of phase. This yields an admixture of dispersion to the absorption depending on the ratio of skin depth and sample size [25, 26].

Figure 3 contains the ESR parameters determined from the fits of the spectra measured in all three crystal directions as a function of the temperature. In the upper panel (a) the resonance field H_{res} is plotted, followed by the g -shift Δg , the signal intensity I_{ESR} , and the linewidth ΔH in the lowest frame (d). The most prominent effect of the metal-insulator transition T_{MI} is visible in the ESR intensity depicted in Fig. 3(c). Resembling the spin susceptibility, in the metallic regime it is Pauli-like, i.e. approx-

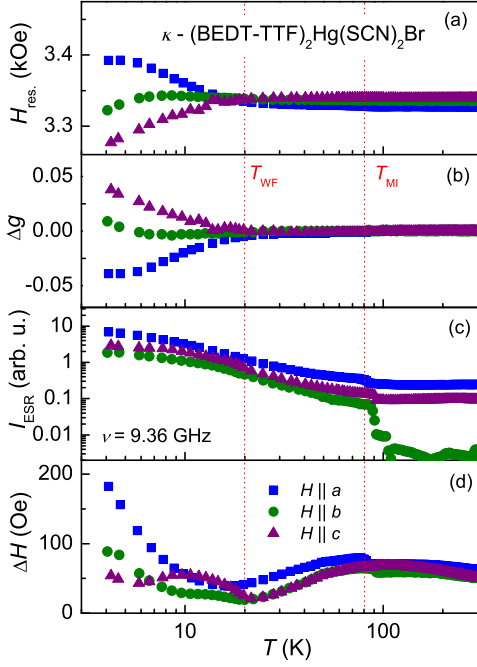


FIG. 3: Temperature dependence of ESR parameters of κ -(BEDT-TTF) $_2$ Hg(SCN) $_2$ Br for the magnetic field applied along the crystallographic principal axes: (a) resonance field H_{res} , (b) g -shift $\Delta g = g - g(300 \text{ K})$, (c) double integrated intensity I_{ESR} , and (d) linewidth ΔH determined at X-band frequency 9.36 GHz. Red dotted lines indicate the metal-insulator transition at $T_{\text{MI}} \approx 80 \text{ K}$ and a weak ferromagnetic transition at $T_{\text{WF}} \approx 20 \text{ K}$.

imately constant; a step indicates the metal-insulator transition at about $T_{\text{MI}} = 80 \text{ K}$. In the insulating regime a pronounced monotonous increase is observed with the tendency for saturation to lowest temperatures. Note that the step is largest for $H \parallel b$ where the microwave field is oscillating perpendicular to the conductive layers, giving rise to the strongest shielding in the metallic regime. The linewidth amounts to about 50 – 60 Oe at room temperature, dependent on the orientation of the sample in the magnetic field, and increases only slightly upon decreasing temperature. As seen in Fig. 3(d), on approaching the metal-insulator transition, ΔH increases abruptly by about 10 Oe and then decreases significantly below $T = 50 \text{ K}$. Finally, for $T < 20 \text{ K}$, one clearly recognizes a strong broadening of ΔH . The resonance fields [Fig. 3(a)] corresponding to g values close to 2 at room temperature ($g_a = 2.011$, $g_b = 2.004$, $g_c = 2.004$) remain nearly unchanged on passing T_{MI} , but develop a strong anisotropy below 20 K, which is even more pronounced considering the g -shift Δg from its respective room-temperature value for each orientation as plotted in Fig. 3(b).

For a quantitative analysis we consider complementary measurements of the static susceptibility χ . In Fig. 4(a), we chose the $\chi \cdot T$ plot in order to elucidate the dif-

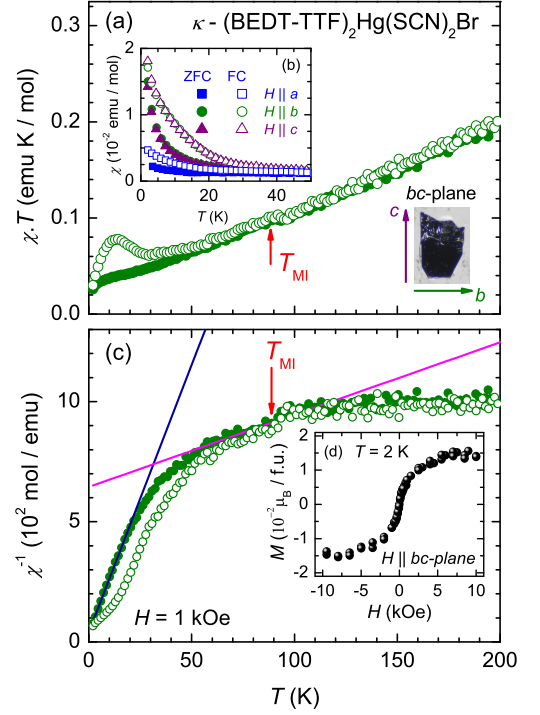


FIG. 4: (a) Temperature dependence of the susceptibility χ of κ -(BEDT-TTF) $_2$ Hg(SCN) $_2$ Br in representation $\chi \cdot T$. (b) $\chi(T)$ for the magnetic field $H = 1 \text{ kOe}$ applied along the three principal crystallographic axes under zero-field cooled (ZFC, solid symbols) and field cooled (FC, open symbols) conditions. The inset depicts the single crystal under investigation. (c) Inverse susceptibility as a function of temperature. Straight lines indicate Curie-Weiss laws as discussed in the text. The inset (d) shows the field dependence of the magnetization at $T = 2 \text{ K}$.

ferent temperature regimes: The strictly linear increase above T_{MI} characterizes the Pauli-like paramagnetism. Just below T_{MI} the descent of the curve is typical for dominant antiferromagnetic exchange interaction. On further decreasing temperature the positive curvature, which for FC conditions is most pronounced and results even in a local maximum of $\chi \cdot T$ below $\approx 20 \text{ K}$, indicates competing ferromagnetic exchange as described e.g. in Ref. 10. Turning to Fig. 4(c), in the temperature range $50 < T < 80 \text{ K}$ the system follows a strongly antiferromagnetic Curie-Weiss law $\chi = C/(T - \Theta_{\text{CW}})$ (magenta line) with a Curie-Weiss temperature $\Theta_{\text{CW}} = -215 \text{ K}$ and a Curie constant $C = 0.33 \text{ emu}/(\text{mol K})$ corresponding to 0.9 electron spins per (BEDT-TTF) $_2$ dimer; hence within the experimental uncertainty all electron spins contribute to the susceptibility. As seen in Fig. 4(b) and (c), ZFC and FC data become distinct when the temperature is reduced below 50 K with a strongly increasing slope. While the ZFC data approach another Curie-Weiss like regime (blue line) with $\Theta_{\text{CW}} = -3 \text{ K}$ and $C = 0.045 \text{ emu}/(\text{mol K})$, the FC data follow an S-shape curve, which finally joins the ZFC data at 2 K.

As shown in the inset of Fig. 4(d), the field-dependent magnetization reveals a soft ferromagnetic loop with a saturation at about $1.5 \times 10^{-2} \mu_B$ per formula unit; a hysteretic behavior could not be identified. Moreover the susceptibility evolves a significant easy-plane anisotropy to low temperatures, as illustrated in Fig. 4(b).

Our comprehensive experimental results on κ -(BEDT-TTF)₂Hg(SCN)₂Br suggest, first, that the metal-insulator transition observed at $T_{MI} \approx 80$ K is not accompanied by long-range magnetic ordering, and second, around $T_{WF} \approx 20$ K a weakly ferromagnetic phase develops. In the following we will discuss these two points.

The Curie-Weiss law observed in the temperature range $50 < T < 80$ K, with all electrons contributing, provide clear evidence that no long-range magnetic order exists below T_{MI} . This behavior is characteristic for a paramagnetic phase of localized spins. The large negative Curie-Weiss temperature indicates strong antiferromagnetic exchange interactions between the spins. While in the case of the Cu- and Ag-based κ -BEDT-TTF salts, $J = 200 - 300$ K is reported [27], for κ -(BEDT-TTF)₂Hg(SCN)₂Br we estimate $J \approx 70$ K from mean-field theory. This value is in a good agreement with that estimated for a dipole solid using a tight-binding approximation ($J = 80$ K) [28]. It was also found by the same authors that the frequency of dipole fluctuations, i.e. the exchange rate between two states, is around 40 cm^{-1} (≈ 86 T). Again this value is in line with our estimation of the exchange field $H_{ex} \approx 78$ T, obtained by Anderson-Weiss molecular-field model [29].

We can definitely rule out any pairing of the spins, as they would not contribute to the susceptibility. Moreover, it is important to note that the g -values do not change at $T_{MI} = 80$ K, i.e. the average position of the electron on the BEDT-TTF₂ molecules does not depend on its mobility. This finding strongly supports the absence of charge order deduced from vibrational spectroscopy [16]. When the electrons become localized, they remain randomly distributed on the (BEDT-TTF)₂ dimers, but do not occupy a certain molecular site.

The triangular structure of the (BEDT-TTF)₂ layers causes strong geometrical frustration of the antiferromagnetic exchange interaction. The fact that both static susceptibility and ESR intensity deviate from the Curie-Weiss law below $T \approx 50$ K indicates some kind of magnetic transition. In particular below 20 K a significant increase of the magnetic susceptibility is observed. The comparison of FC and ZFC susceptibilities and ESR spectra as well as the field dependence of the magnetization at low temperature indicates a weak ferromagnetic polarization. Additionally, the g -values reveal an increasing anisotropy below 20 K accompanied by inhomogeneous line broadening. Indeed the shift of the resonance field to higher fields (negative g -shift) for $H \parallel a$, i.e. perpendicular to the platelet shaped crystal, as well as the opposite behavior for the magnetic field applied within the

bc -plane are typical signs for demagnetization effects in ferromagnetic platelets.

Let us return to the field dependent magnetization measurements, indicating a saturation around $15 \times 10^{-3} \mu_B$ /formula unit. This value is one order of magnitude larger than that in κ -(BEDT-TTF)₂Cu[N(CN)₂]Cl ($8 \times 10^{-4} \mu_B$ /formula) [30], which was interpreted as a canted antiferromagnet. Below $T_N = 27$ K that compound orders antiferromagnetically [31]; however, the ordering is accompanied by weak ferromagnetism due to the canting of the antiparallel spins [30]. Multi-frequency ESR measurements identified a paramagnetic resonance but also the shift to the antiferromagnetic resonance below T_N [33–35]. The antiferromagnetic modes can be well explained only by taking into account the Dzyaloshinsky and Moriya interaction [36–40]. However neither such antiferromagnetic mode nor the separation of any high-frequency mode at the ordering temperature has been observed in κ -(BEDT-TTF)₂Hg(SCN)₂Br. Therefore, we conclude that in the present case another mechanism drives the weak ferromagnetism.

To unravel the underlying mechanism, we recall that in κ -(BEDT-TTF)₂Hg(SCN)₂Br frustration – due to the triangular lattice – and disorder – due to the absence of charge order and random localization – are both present; hence, a spin-glass-like ground state can be expected as sketched in Fig. 1. Indeed frustration impedes antiferromagnetic order; and disorder is able to drive weak ferromagnetism. These conclusions are supported by the model of McConnell [41], who proposed a theory for spin-density – spin-density interaction in a stack of π -electron molecules. He considered the spin Hamiltonian for a pair of molecules. Due to the spin polarization, positive and negative spin densities are found in different atoms of each molecule. It was seen that when the molecules are exactly stacked on each other, the intermolecular exchange energy becomes negative when the spins of a pair of molecules are antiparallel, that is, the molecules are antiferromagnetically coupled. On the other hand, when the atoms of positive spin density of one molecule are most strongly coupled to atoms of negative spin density in the neighbor, the intermolecular interaction energy becomes negative for parallel spins. The stacked molecules are then ferromagnetically coupled to each other. With other words weak ferromagnetism arises from the disorder due to random localization of the electrons on the (BEDT-TTF)₂ dimers, i.e. the general antiferromagnetic exchange is modulated by disorder in the spin density on each molecular dimer, thus giving rise to locally ferromagnetic alignment of neighboring spins.

To summarize our ESR and susceptibility study of κ -(BEDT-TTF)₂Hg(SCN)₂Br, on passing the metal-insulator transition at $T_{MI} \approx 80$ K, the conduction electrons localize at the (BEDT-TTF)₂ molecular dimers, but – different from a Mott transition – without formation of long-range antiferromagnetic order. Instead, ge-

ometric frustration keeps the antiferromagnetically coupled spin system in a paramagnetic state, as proven by the Curie-Weiss law of the susceptibility. Below about $T_{WF} \approx 20$ K a weakly ferromagnetic behavior shows up. Taking into account that there is no charge order below T_{MI} , disorder in the related spin-density of neighboring (BEDT-TTF)₂ molecular dimers locally gives rise to ferromagnetic interactions. Regarding the field-cooling induced enhancement of the susceptibility at low temperatures, we suggest the evolution of a weakly ferromagnetic spin-glass state below T_{WF} resulting from geometric frustration within the (BEDT-TTF)₂ layers and disorder of charge and spin density on each (BEDT-TTF)₂ molecular dimer.

This work was supported by the Deutsche Forschungsgemeinschaft (DFG) by DR228/39-1 and DR228/52-1, as well as the Transregional Collaborative Research Center TRR 80 (Augsburg-Munich-Stuttgart).

-
- [1] O. Kahn, *Molecular Magnetism*, VCH Publishers Inc., New York (1993).
- [2] T.P. Radhakrishnan, *Current Science* **62**, 669 (1992).
- [3] J. S. Miller and M. Drillon, *Magnetism: Molecules to Materials* (Vol. I – V), Wiley-VCH, Weinheim (2001).
- [4] D. Gatteschi, R. Sessoli, and J. Villain, *Molecular Nanomagnets* Oxford University Press, Oxford (2006).
- [5] Z. Soos, *Annu. Rev. Phys. Chem.* **25**, 121 (1974).
- [6] S. J. Blundell and F. L. Pratt, *J. Phys.: Condens. Matter* **16**, R771 (2004).
- [7] E. C. Stoner, *Magnetism*, Methuen and Co (1930); J.B. Goodenough, *Magnetism and chemical bond*, Interscience Publishers, New York (1963); C. Zener, *Phys. Rev.* **82**, 403 (1951).
- [8] T. Ishiguro, K. Yamaji, and G. Saito, *Organic Superconductors*, 2nd edition (Springer-Verlag, Berlin, 1998).
- [9] N. Toyota, M. Lang, and J. Müller, *Low-Dimensional Molecular Metals* (Springer-Verlag, Berlin, 2007).
- [10] T. Mori, *Electronic Properties of Organic Conductors*, Spinger-Verlag, Berlin (2016).
- [11] B. J. Powell and R. H. McKenzie, *Rep. Prog. Phys.* **74**, 056501 (2011).
- [12] K. Kanoda, *Hyperfine Interact.* **104**, 235 (1997); *J. Phys. Soc. Japan* **75**, 051007 (2006).
- [13] A. Pustogow, M. Bories, A. Löhle, R. Rsslhuber, E. Zhukova, B. Gorshunov, S. Tomić, J.A. Schlueter, R. Hübner, T. Hiramatsu, Y. Yoshida, G. Saito, R. Kato, S. Fratini, T.-H. Lee, V. Dobrosavljević and M. Dressel, submitted to *Nature Materials* (2017)
- [14] R. B. Lyubovskii, R. N. Lyubovskaya, O. A. Dyachenko, *J. Phys. I (France)* **6**, 1609 (1996).
- [15] N. Drichko, R. Beyer, E. Rose, M. Dressel, J. A. Schlueter, S. A. Turunova, E. I. Zhilyaeva, and R. N. Lyubovskaya, *Phys. Rev. B* **89**, 075133 (2014).
- [16] T. Ivek, R. Beyer, S. Badalov, M. Čulo, S. Tomić, J. M. Schlueter, E. I. Zhilyaeva, R. N. Lyubovskaya, and M. Dressel, *Phys. Rev. B* **96**, 085116 (2017).
- [17] A. Löhle, E. Rose, S. Singh, R. Beyer, E. Tafra, T. Ivek, E. I. Zhilyaeva, R. N. Lyubovskaya, and M. Dressel, *J. Phys.: Condens. Matter* **29**, 055601 (2017).
- [18] K. Sedlmeier, S. Elsässer, D. Neubauer, R. Beyer, D. Wu, T. Ivek, S. Tomić, J. A. Schlueter, and M. Dressel, *Phys. Rev. B* **86**, 245103 (2012).
- [19] M. Pinterić, P. Lazić, A. Pustogow, T. Ivek, M. Kuveždić, O. Milat, B. Gumhalter, M. Basletić, M. Čulo, B. Korin-Hamzić, A. Löhle, R. Hübner, M. Sanz Alonso, T. Hiramatsu, Y. Yoshida, G. Saito, M. Dressel, S. Tomić, *Phys. Rev. B* **94**, 161105 (2016).
- [20] E. I. Yudanov, S. K. Hoffmann, A. Graja, S. V. Konovalikhin, O. A. Dyachenko, R. B. Lyubovskii, R. N. Lyubovskaya, *Synthetic Metals* **73**, 227 (1995).
- [21] S. V. Konovalikhin, G. V. Shilov, O. A. Dyachenko, M. Z. Aldoshina, R. N. Lyubovskaya, and R. B. Lyubovskii, *Bull. of Russ. Acad. Sci.: Phys.* **41**, 903 (1992).
- [22] M. Z. Aldoshina, R. N. Lyubovskaya, S. V. Konovalikhin, O. A. Dyachenko, G. V. Shilov, M. K. Makova, and R. B. Lyubovskii, *Synth. Met.* **55**, 1905 (1993).
- [23] K. G. Padmalekha, M. Blankenhorn, T. Ivek, L. Bogani, J. A. Schlueter, and M. Dressel, *Physica B* **460**, 211 (2015).
- [24] R. V. Upadhyay, K. Parekh, and R. V. Mehta, *Phys. Rev. B* **68**, 224434 (2003).
- [25] S. E. Barnes, *Adv. Phys.* **30**, 801 (1981).
- [26] J. P. Joshi and S. V. Bhat, *J. Magn. Reson.* **168**, 284 (2004).
- [27] Y. Shimizu, K. Miyagawa, K. Kanoda, M. Maesato, and G. Saito, *Phys. Rev. Lett.* **91**, 107001 (2003); Y. Shimizu, T. Hiramatsu, M. Maesato, A. Otsuka, H. Yamochi, A. Ono, M. Itoh, M. Yoshida, M. Takigawa, Y. Yoshida, and G. Saito, *Phys. Rev. Lett.* **117**, 107203 (2016).
- [28] N. Hassan, S. Cunningham, M. Mourigal, E. I. Zhilyaeva, S. A. Torunova, R. N. Lyubovskaya, N. Drichko, arXiv:1704.04482v2 (2017).
- [29] P. W. Anderson and P. R. Weiss, *Rev. Mod. Phys.* **25**, 269 (1953).
- [30] U. Welp, S. Fleshler, W. K. Kwok, G. W. Crabtree, K. D. Carlson, H. H. Wang, U. Geiser, J. M. Williams, and V. M. Hitsman, *Phys. Rev. Lett.* **69**, 840 (1992).
- [31] K. Miyagawa, A. Kawamoto, Y. Nakazawa, and K. Kanoda, *Phys. Rev. Lett.* **75**, 1174 (1995).
- [32] M. Pinterić, M. Miljak, N. Biškup, O. Milat, I. Aviani, S. Tomić, D. Schweitzer, W. Strunz, and I. Heinen, *Eur. Phys. J. B* **11**, 217 (1999).
- [33] M. Kubota, G. Saito, H. Ito, T. Ishiguro, N. Kojima, *Mol. Cryst. Liq. Cryst.* **284**, 367 (1996).
- [34] H. Ohta, S. Kimura, Y. Yamamoto, J. Azuma, K. Akioka, M. Motokawa and K. Kanoda, *Synthetic Metals* **86**, 2079 (1997).
- [35] H. Ohta, N. Nakagawa, K. Akioka, Y. Nakashima, S. Okubo, K. Kanoda, and N. Kitamura, *Synthetic Metals* **103**, 1914 (1999).
- [36] D. Smith, S. De Soto, C. Slichter, J. Schlueter, A. Kini, and R. Daugherty, *Phys. Rev. B* **68**, 024512 (2003).
- [37] F. Kagawa, Y. Kurosaki, K. Miyagawa, and K. Kanoda, *Phys. Rev. B* **78**, 184402 (2008).
- [38] Á. Antal, T. Fehér, B. Náfrádi, L. Forró, and A. Jánossy, *J. Phys. Soc. Jpn.* **84**, 124704 (2015).
- [39] I. Dzyaloshinsky, *J. Phys. Chem. Solids* **4**, 241 (1958).
- [40] T. Moriya, *Phys. Rev.* **120**, 91 (1960).
- [41] H. M. McConnell, *J. Chem. Phys.* **39**, 1910 (1963).